

Elucidating Ionic Correlations Beyond Simple Charge Alternation in Molten MgCl₂-KCl Mixtures

F. Wu, E. Dooryhee

To be published in "JOURNAL OF PHYSICAL CHEMISTRY LETTERS"

November 2019

Photon Sciences

Brookhaven National Laboratory

U.S. Department of Energy

USDOE Office of Science (SC), Basic Energy Sciences (BES) (SC-22)

Notice: This manuscript has been authored by employees of Brookhaven Science Associates, LLC under Contract No. DE-SC0012704 with the U.S. Department of Energy. The publisher by accepting the manuscript for publication acknowledges that the United States Government retains a non-exclusive, paid-up, irrevocable, world-wide license to publish or reproduce the published form of this manuscript, or allow others to do so, for United States Government purposes.

DISCLAIMER

This report was prepared as an account of work sponsored by an agency of the United States Government. Neither the United States Government nor any agency thereof, nor any of their employees, nor any of their contractors, subcontractors, or their employees, makes any warranty, express or implied, or assumes any legal liability or responsibility for the accuracy, completeness, or any third party's use or the results of such use of any information, apparatus, product, or process disclosed, or represents that its use would not infringe privately owned rights. Reference herein to any specific commercial product, process, or service by trade name, trademark, manufacturer, or otherwise, does not necessarily constitute or imply its endorsement, recommendation, or favoring by the United States Government or any agency thereof or its contractors or subcontractors. The views and opinions of authors expressed herein do not necessarily state or reflect those of the United States Government or any agency thereof.

Elucidating Ionic Correlations Beyond Simple Charge Alternation in Molten MgCl₂-KCl Mixtures

Fei Wu,[†] Santanu Roy,[‡] Alexander S. Ivanov,^{*,‡} Simerjeet K. Gill,[%] Mehmet Topsakal,[%] Eric Dooryhee,^{††} Milinda Abeykoon,^{††} Gihan Kwon,^{††} Leighanne C. Gallington,[§] Phillip Halstenberg,^{‡,#} Bobby Layne,[&] Yoshiki Ishii,[◇] Shannon M. Mahurin,[‡] Sheng Dai,[‡] Vyacheslav S. Bryantsev,^{*,‡} Claudio J. Margulis^{*,†}

AUTHOR INFORMATION

[†]Department of Chemistry, The University of Iowa, Iowa City, IA 52242, USA

[‡]Chemical Sciences Division, Oak Ridge National Laboratory, Oak Ridge, TN 37831, USA.

[%]Nuclear Science and Technology Department, Brookhaven National Lab, Upton, NY 11973

^{††}National Synchrotron Light Source II (NSLS-II), Brookhaven National Laboratory, Upton, NY 11973, USA

[§]X-ray Science Division, Advanced Photon Source, Argonne National Laboratory, Argonne, IL 60439, USA.

[#]Dept. of Chemistry, University of Tennessee, Knoxville, TN 37996

[&]Chemistry Division, Brookhaven National Laboratory, Upton, NY 11973-5000

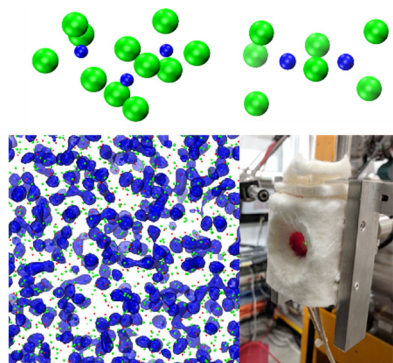
[◇]Division of Chemical Engineering, Graduate School of Engineering Science, Osaka University, 1-3 Machikaneyama, Toyonaka, Osaka 560-8531, Japan

Corresponding Author

ivanova@ornl.gov, bryantsevv@ornl.gov, claudio-margulis@uiowa.edu

ABSTRACT: The development of technologies for nuclear reactors based on molten salts has seen a big resurgence. The success of thermodynamic models for these hinges in part on our ability to predict at the atomistic level the behavior of pure salts and their mixtures under a range of conditions. In this letter, we present high-energy X-ray scattering experiments and Molecular Dynamics simulations that describe the molten structure of mixtures of MgCl_2 and KCl . As one would expect, KCl is a prototypical salt in which structure is governed by simple charge alternation. In contrast, MgCl_2 and its mixtures with KCl display more complex correlations including intermediate-range order and the formation of Cl^- -decorated Mg^{2+} chains. A thorough computational analysis suggests that intermediate-range order beyond charge alternation may be traced to correlations between these chains. An analysis of the coordination structure for Mg^{2+} ions paints a more complex picture than previously understood, with multiple accessible states of distinct geometries.

TOC GRAPHICS



KEYWORDS Molten Chloride Salts, MgCl₂, KCl, X-ray Scattering, Simulations.

Driven by the challenge to find sustainable and safe sources of energy, molten salts have re-emerged as potential coolants in nuclear reactors five decades since the concept was successfully demonstrated.¹⁻⁹ Because of their minimal vapor pressure¹⁰⁻¹⁵ when compared to water, such systems present many advantages including their potential operation near ambient pressure. Chloride-containing molten salts are intriguing and potentially advantageous for certain applications,¹⁶⁻¹⁹ including the development of new generation fast-spectrum molten salt reactors, where chloride salts are preferentially used over fluorides because of their higher atomic weight and reduced moderating capacity.²⁰⁻²¹ Consequently, mixtures of MgCl₂ with KCl and/or NaCl are considered to be promising media for Pu(U)Cl₃-based fuel salts.^{20,22} There are engineering models that predict bulk thermodynamic properties of molten salts,²³⁻²⁴ yet, major gaps still exist in our understanding of ionic coordination numbers used as input in these models, intermediate range order, and molten salt interactions with materials in general. The reason why understanding structure (including intermediate range order and coordination environments) is important to thermodynamics, has to do with the activity coefficients and chemical/electrochemical potentials of the ions.²⁵⁻²⁷ Specifically, the expectation is that order on multiple scales will affect Lewis acidities or basicities of the ions due to long-range Coulombic interactions; as an example, whereas MgCl₂ readily dissolves UO₂, CaCl₂ does not.²⁷

Early pioneering works on pure MgCl₂ molten salt exist, and particularly relevant and noteworthy are the neutron scattering study by Biggin *et al.*²⁸ and the theoretical work by Wilson and Madden.²⁹ In the latter, insightful were arguments on whether models including covalent bonding were necessary to capture correct inter-ionic distances or if these could be properly

recovered by the inclusion of ionic polarizabilities. Using a simple but very effective polarizable ion model that succeeded where other shell-based models or rigid ion models did not, the authors were able to create a generic description of divalent molten salts. A few early Raman spectroscopy studies³⁰⁻³⁷ are also very important, as they attempted to describe the type of associations and geometries present in the molten states of MgCl₂ and its mixtures with KCl. As will become apparent during the presentation of our X-ray scattering and simulation results, many of the earlier findings and their interpretation still hold valid, but other concepts accepted as facts for decades may need further scrutiny. For example, the accepted concept of tetrahedral coordination associated with Mg²⁺ in the molten state, as well as the concomitant interpretation of intermediate-range order based on it, require revisiting. This is to be expected, as pioneering scattering experiments were limited in the range of momentum transfer (q) values they could probe.

Synchrotron X-ray scattering data on molten MgCl₂-KCl mixtures (15% MgCl₂-85% KCl, 35% MgCl₂-65% KCl and 50% MgCl₂-50% KCl mole fractions) were collected at 1073 K using a customized furnace (Figure 1a) specifically constructed to hold a sample in quartz capillaries at high temperature. Figure 1b provides a comparison between X-ray structure functions ($S(q)$) against those derived from our *ab-initio* molecular dynamics (AIMD) and polarizable ion model (PIM)³⁸⁻⁴⁰ molecular dynamics (MD) (section 1 in the SI, and in particular Figures S.1 through S.7, describe in detail our experimental setup and protocols; section 2 provides details of our computational protocols). In addition, Figure S.8 shows experimentally derived structure functions in their full reciprocal space range up to 20 Å⁻¹. For pure MgCl₂ in the molten state, we also provide in Figure S.9 a comparison between our simulation results and data digitized and reanalyzed based on the original neutron data by Biggin *et. al.*²⁸ In all cases, our $S(q)$ derived from MD simulations

agrees reasonably well with that obtained from the scattering data providing confidence in our analysis of structural correlations based on them.

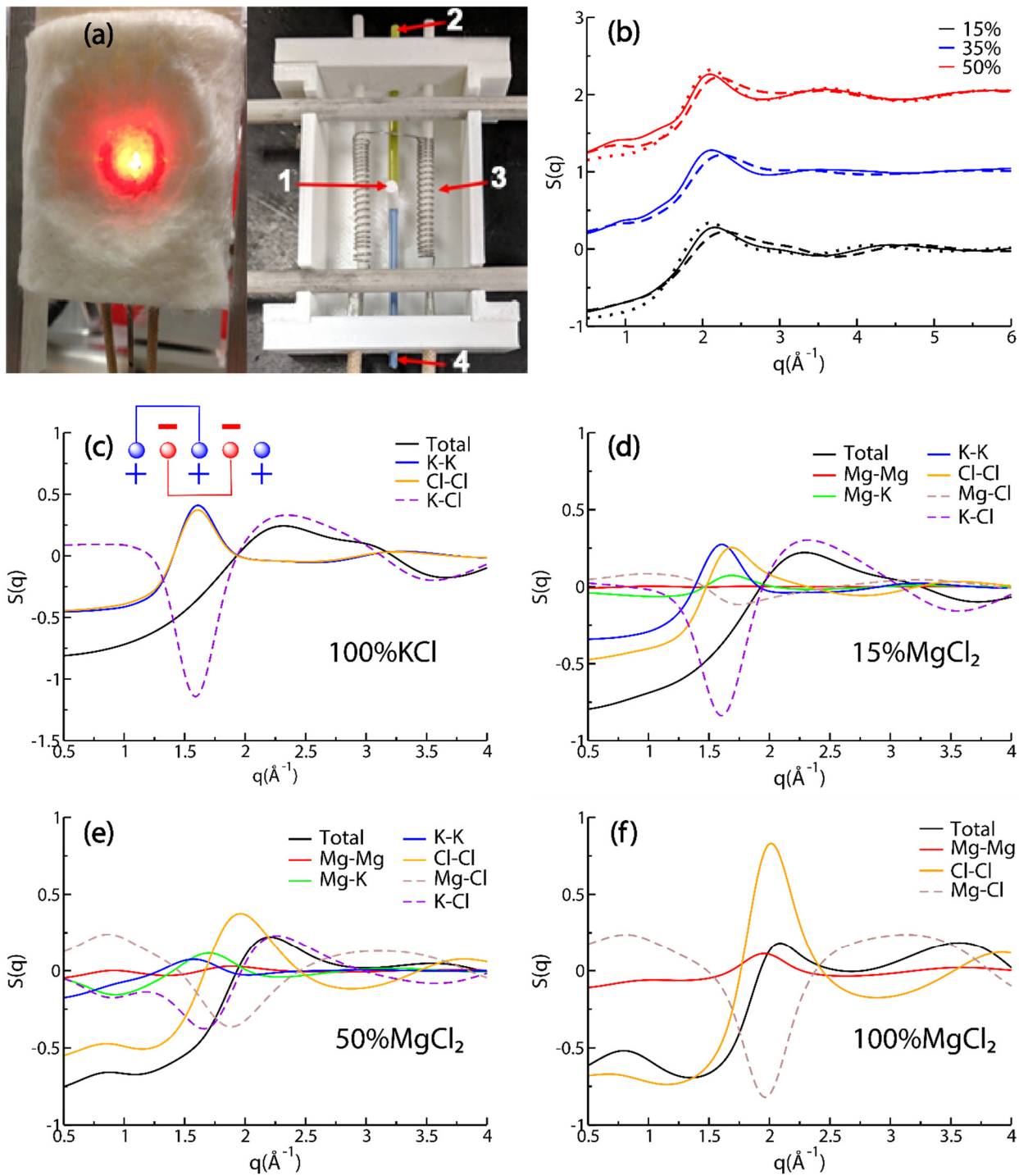


Figure 1. (a) Furnace used for the high-temperature X-ray scattering experiments: (1) X-ray entrance port, (2) sample port, (3) heating wire, (4) thermocouple port. (b) The structure functions for three different MgCl₂-KCl mole fractions of molten salts: 15% MgCl₂-85% KCl (black), 35% MgCl₂-65% KCl (blue) and 50% MgCl₂-50% KCl (red). X-ray scattering measurements (solid lines), AIMD simulations (dots), and PIM simulations (dashes) at 1073 K. Total and partial subcomponents of S(q) from our PIM simulations at 1073 K for (c) pure KCl, (d) 15% MgCl₂ mixture, (e) 50% MgCl₂ mixture and (f) pure MgCl₂. An inset in (c) highlights the charge-alternation region. Structure functions in (c) through (f) are shown in a limited q range since q values beyond 4 Å⁻¹ correspond to approximate real space distances (2π/q) shorter than a typical inter-ionic distance.

From Figure 1b we see that for the most part, the agreement between AIMD results and experiments is excellent above 1.5 Å⁻¹, but box size limitations restrict their accuracy at lower q values. Instead, using larger simulation boxes with the PIM model affords reasonable reproduction of experimental features across the full range of relevant q values. By partitioning S(q) into different ionic subcomponents (Figures 1c through 1f), we can interpret the underlying molten salt structure. In order to trace how the scattering profile changes upon the addition of MgCl₂ to the mixture, we focus first on the partitions of S(q) for pure KCl (Figure 1c). The total S(q) shows prominent peaks above 2 Å⁻¹ that in this case more or less mimic the behavior of the K-Cl cross S(q) subcomponent. These peaks correspond to what in prior work we have labeled adjacency correlations.⁴¹⁻⁴² Since it is opposite-charge ions that are most commonly found at close contact distance, it is not unexpected that adjacency correlations may be dominated by the K-Cl subcomponent of S(q).

The most important characteristic of all molten salts is charge alternation, which always manifests in partitions of $S(q)$ as positive-going peaks in the case of same-charge ions and negative going peaks (which we have termed in prior work “antipeaks”⁴³⁻⁴⁴) for opposite-charge ions. In a simple prototypical salt like KCl, one always expects two peaks (corresponding to positive-positive and negative-negative correlations) and one antipeak (corresponding to positive-negative correlations) at about the same q value. This pattern can be clearly observed in Figure 1c slightly above 1.5 \AA^{-1} where the K-K and Cl-Cl correlations appear as peaks but the K-Cl correlation appears as an antipeak.

We emphasize that this pattern is the hallmark of all molten salts (and ionic liquids in general), however, it is often concealed in the total experimental $S(q)$ because of perfect cancellations of peaks and antipeaks. For example, in the total $S(q)$ for KCl, the charge alternation peak is completely missing. This is not because positive-negative ion alternation is absent in the melt but instead because of perfect cancellations or what is commonly referred to as “lack of contrast”. This is the reason why simulations are so important in revealing the underlying bulk phase structure.

We now focus on the pure salt MgCl_2 , for which partial subcomponents of $S(q)$ are depicted in Figure 1f. For MgCl_2 , the charge alternation pattern is present at about 2 \AA^{-1} . This is obvious from the Cl-Cl and Mg-Mg peaks at the q range where one observes the Mg-Cl antipeak. At larger q values, we still have the adjacency correlations whereas at smaller q values we have a feature below 1 \AA^{-1} , which is commonly referred to as a prepeak or a first sharp diffraction peak.^{41-42, 45}

Whereas the pattern in the subcomponents of $S(q)$ for charge alternation is quite universal and simple to detect, determining the origin of the prepeak is very challenging. Notice that in contrast to the case for KCl where the charge alternation peak is completely masked in the total $S(q)$, it is instead prominently present for MgCl_2 . This has no special meaning, since both salts are dominated

by charge alternation –this is just a contrast issue. However, there is a cautionary tale here; without computationally splitting $S(q)$ into subcomponents it would have been easy to mistakenly assume that the adjacency peak in the experimental $S(q)$ above 2 \AA^{-1} for KCl had the same origin as the charge alternation peak at the same q range for MgCl_2 . This would have been wrong.

Figures 1d and 1e show a much more complex situation since multiple ions are present in the high-temperature melt. Yet, the pattern of adjacency and more interestingly charge alternation (peaks for same-charge ions K-K, Mg-K, Cl-Cl and antipeaks for the opposite-charge ions K-Cl and Mg-Cl) can be easily identified, each of them slightly shifted due to the different ionic sizes. Similar to pure MgCl_2 , the 50% mixture also displays a clear prepeak below 1 \AA^{-1} . Figure S.10 in the SI shows the progression of the total $S(q)$ across a larger mole fraction range highlighting the development of the prepeak at low q values as the mole fraction of MgCl_2 becomes dominant.

Because the prepeak reveals patterns on longer length scales (low q) instead of shorter-range alternations, it is perhaps more illustrative to begin our description in real space. Figures 2a through 2c show snapshots from simulation where the mole fraction of MgCl_2 is 15%, 50% and 100%. Highlighted as blue isosurfaces is a 3D Fourier expansion of the density⁴⁶ of Mg^{2+} ions. Whereas the choice of isovalue is somewhat arbitrary, it is clear from this figure that at low mole fraction, Mg^{2+} ions appear disconnected. As the mole fraction increases to 50%, short Mg^{2+} chains or clusters are formed and at 100% mole fraction these chains become longer.

How is it possible that small dipositive ions become sufficiently close to form networks? Figure S.11 shows real space radial distribution functions for the different ions. A key qualitative aspect of these distributions was already understood and nicely highlighted in the early work by Wilson and Madden – the first peak in $g(r)$ for Mg-Mg overlaps with that for Cl-Cl.²⁹ The significant polarizability of chloride ions is crucially important to achieve this. Without polarizability, the

distance between two dipositive ions should be significantly larger than between two Cl^- ions. If shorter distances between dipositive ions were physically disallowed, the chains of Mg^{2+} ions decorated by Cl^- anions that we observe could not form and each Mg^{2+} would necessarily form its own distinct “complex” with Cl^- ions. Since at lower Mg^{2+} mole fractions our molten salt mixtures do not show a prepeak in $S(q)$, it would be intuitive to assume that the prepeak has to do with the formation of networks. In other words, in situations such as Figure 2a where each Mg^{2+} ion is fully solvated by counterions without other Mg^{2+} nearby, there is no prepeak. This is correct, but the origin of the prepeak is more nuanced.

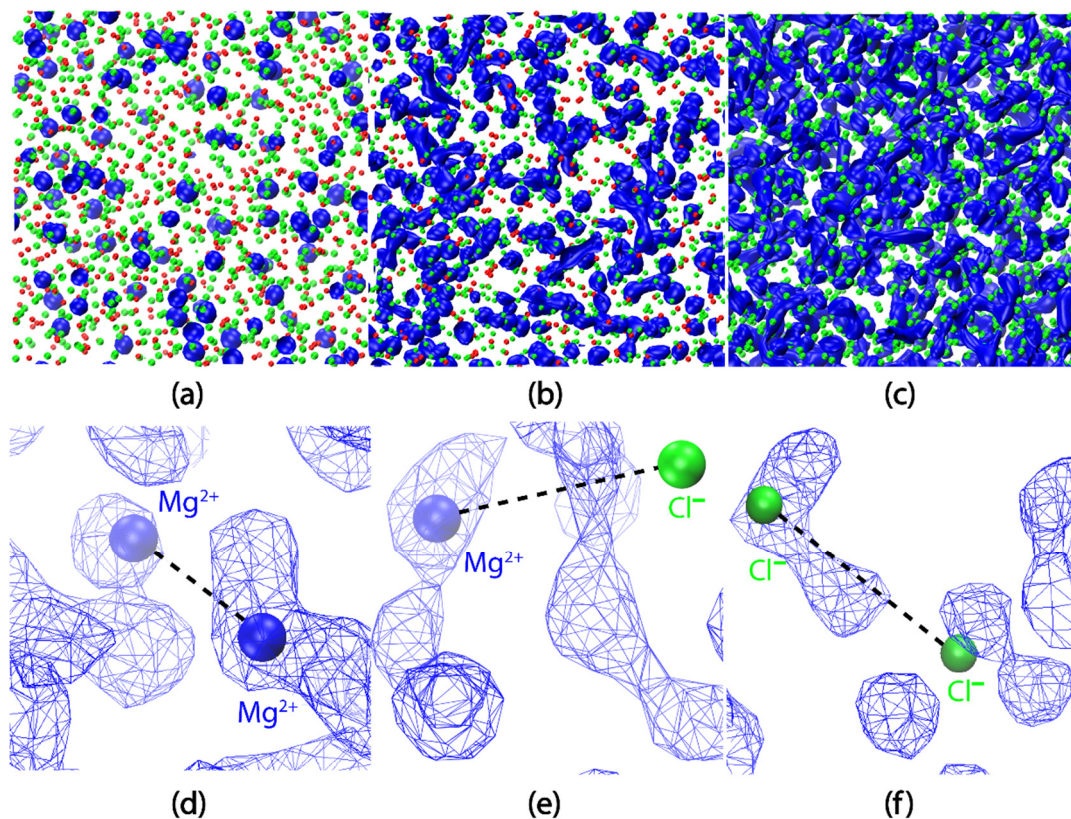


Figure 2. (a) through (c) Snapshots at 15%, 50% and 100% in MgCl_2 from our larger PIM box simulations at 1073 K. Cl^- , green; K^+ , red; Mg^{2+} , blue spheres (enclosed inside blue isosurfaces). Ion radii are depicted not to scale to better highlight the Mg^{2+} network extent. Notice that snapshots match the behavior seen in the first peak of the Mg-Mg pair distribution functions in Figure S.12,

were low intensity is associated with low Mg^{2+} mol fraction and the absence of networks. (d) through (f) are examples of ion pair interactions with important contribution to the prepeak.

To get at the origin of the prepeak we resort to computing $S(q)$ as a sum over ionic pairs instead of the Fourier transform of the pair distribution functions $g(r)$. For a given simulation frame we can inquire which pair of ions contributes significantly to $S(q)$ while also being at distances approximately resonant with the Bragg condition $d \approx 2\pi/q$ (see section 2.3 in reference⁴⁷ and in particular equation 6). We find that many of the important contributions to the prepeak satisfying the Bragg condition come not from in-chain correlations --the blue isosurfaces in Figures 2b and 2c--, but instead from correlations between ions that are part of or that decorate different but adjacent networks (in some cases correlations are between a network and a single Mg^{2+} complex that does not belong to the same network); examples are shown in Figures 2d, 2e and 2f. Put differently, networks exist when the prepeak occurs, but it is not necessarily the in-network correlations but instead the across-network correlations that may be most important. More intense prepeaks are associated with a larger density of such across network spatial correlations which become a repetitive pattern in the liquid as can be seen from Figure 2c.

The behavior in the liquid phase is somewhat reminiscent of what one observes in the case of crystalline MgCl_2 . Figure 3a overlays the simulated coherent X-ray intensity derived from $S(q)$ in the molten phase with the Bragg peaks in the solid; Figures 3b through 3e show examples of planes associated with the type of interactions we have described in this letter (as well as prior publications^{41, 44, 48-50}) as adjacency correlations, charge alternation and the prepeak. We see from Figure 3b that the (0 0 3) plane --the lowest q peak in the crystal phase-- is related to the distance between parallel magnesium networks decorated by chloride ions. This is essentially the same qualitative behavior we observe for the prepeak, which is the lowest q peak in the molten phase.

Obviously, the crystal networks are parallel and infinitely long, whereas in the melt they are shorter and randomly oriented as can be gleaned from Figure 2. Yet, the origin of the prepeak in the melt appears also to be associated with between-network interactions.

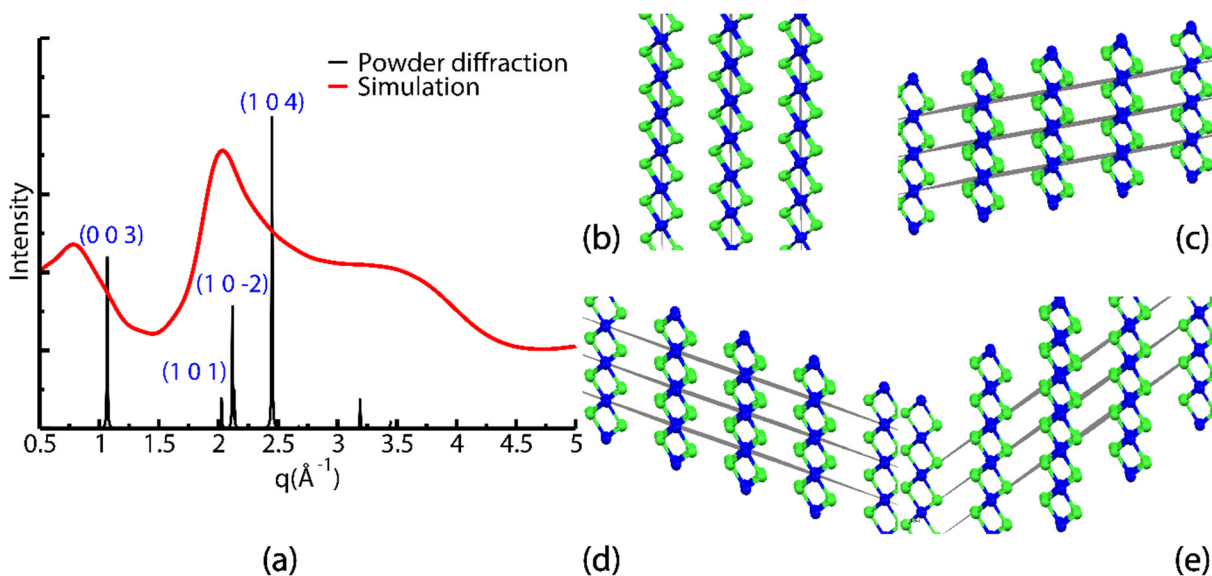


Figure 3. (a) Powder diffraction peaks from reference⁵¹ for MgCl₂ at room temperature as compared with the coherent intensity for molten MgCl₂ at 1073 K from our larger box PIM simulations. (b) (0 0 3) (c) (1 0 -2) (d) (1 0 1) and (e)(1 0 4) Bragg planes in the MgCl₂ crystal. The first set of planes exemplifies across network --prepeak behavior--, the second two are examples of charge alternation behavior, whereas the last set of planes exemplify what in the molten state we would call adjacency correlations.

Since they correspond to typical distances between Mg²⁺ ions when there are Cl⁻ ions between them, we see from Figure 3c and 3d that planes (1 0 1) and (1 0 -2) match what we have described in the melt as the charge alternation peak. Whereas from Figure 3e we see that (1 0 4) is part of the family of planes we have described in the melt as adjacency correlations representing the typical structural interactions between ions that are in contact.

In the early literature on MgCl_2 ,^{28-31, 33, 35, 52-57} significant attention was given to the issue of nearest-neighbor coordination of Mg^{2+} . Even then, it was clearly understood that this quantity was ill-defined in the sense that it significantly depended on the criterion used to define the limits of integration for the pair distribution function.⁵⁸ For example, for NaCl, Biggin and Enderby proposed that this number was 3.9 ± 0.2 for one method and 5.3 ± 0.4 for a different method.⁵² In the case of MgCl_2 , their originally reported coordination number for Mg^{2+} (by defining the criterion of the maximum r for integration as the minimum of value of the function ($r^*g(r)$) assuming this function is symmetric about its first maximum) was 4.3 ± 0.3 . In their study,²⁸ $g(r)$ was derived from back Fourier transformation of their neutron scattering data.

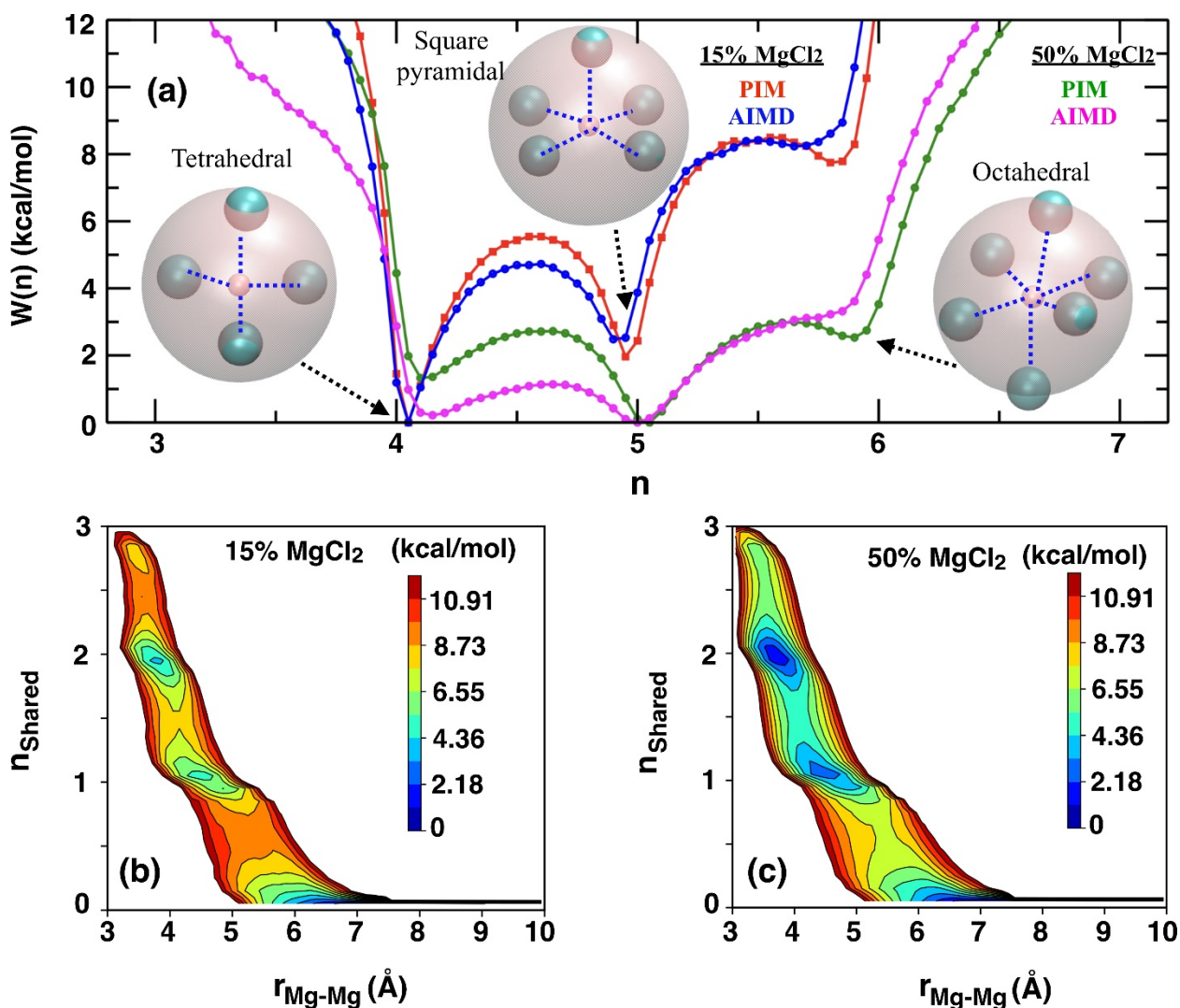


Figure 4. (a) Free energy profiles ($W(n)$) highlighting structural elements in coordination number space obtained from first principles and PIM simulations at 1073 K. The free energies ($W(r, n_{\text{Shared}})$) for (b) 15% and (c) 50% of MgCl_2 , as a function of inter Mg-Mg distance and number of shared chloride ions. For consistency, all results are based on our smaller box simulations (see figure on right of Table S2 showing negligible dependence on box size for the free energy).

Whereas those isotopically-labeled neutron scattering studies were truly pioneering, the inverse Fourier transformation to generate pair distribution functions was necessarily limited by the maximum q value experimentally accessible. Prior work suggests that truncation may lead to shorter and broader first $g(r)$ peaks, which is problematic for the definition of coordination number.⁵⁹⁻⁶⁰ In subsequent studies citing the Biggin and Enderby experiments, the 4.3 ± 0.3 coordination number for chlorides around a magnesium cation was commonly assumed to be 4.^{29, 53, 57, 61-62} This supported some early Raman studies implying tetrahedrality in the molten state for this salt.^{32-33, 35-36} This was quite exciting at the time, since it implied that the molten state was quite different in terms of coordination number when compared to the crystal where coordination is by 6 chloride ions.

Our first principles and classical polarizable simulations which (1) match well our X-ray scattering data for the MgCl_2 -KCl mixtures, and (2) also match well the original Biggin and Enderby neutron scattering data²⁸ (see Figure S.9 in the SI) paint a slightly different story. Figure 4a shows that a significant fraction of the Mg^{2+} ions are in a four-coordinated, tetrahedral geometry. This is particularly the case when the mole fraction of Mg^{2+} is low. However, the four-coordinate structure does not appear to be the most populous state at larger MgCl_2 mole fractions. Instead, the five-coordinate structure is the most likely and we also observe a fraction of six-

coordinate structures as well (probability values are provided in Table S2). These results support reverse Monte Carlo studies by McGreevy where the distribution of Cl^- around Mg^{2+} was described as an octahedron with one Cl^- missing.⁵⁶ The four-, five- or six-coordinated ions should not be seen as complexes in isolation since many are part of chloride-decorated magnesium chains such as depicted in Figure 2, particularly at higher mole fractions. This is emphasized in Figures 4b and 4c where a 2-D free energy landscape is shown as a function of the number of chloride ions shared by magnesium ions and as a function of their interionic distance. From Figure 4b we see that at low magnesium mole fraction the most likely state is consistent with Mg^{2+} ions that are far apart and share no anions. The reader is encouraged to see this in the context of Figure 2a and the fact that at low Mg^{2+} mole fraction there is no prepeak in $S(q)$ (see Figure 1). Instead, Figure 4c shows a prominent minimum at short Mg-Mg distance consistent with the first peak in the Mg-Mg pair distribution function in Figure S.12. Associated with this free energy minimum are two chloride ions shared by the pair of Mg^{2+} ions. These chlorides are commonly seen at the waist of adjacent magnesium ions forming chains in Figure 2b.

In conclusion, our experimental and computational studies highlight that molten mixtures of MgCl_2 and KCl display complex structural behavior on multiple length-scales. At short range, the coordination number of anions and local structure around Mg^{2+} is dependent on the fraction of MgCl_2 . At intermediate length scales, dependent on the mole fraction of Mg^{2+} ions, these can be mostly dissociated or form anion-decorated networks. The proximity of Mg^{2+} networks, linked to their high density, appears to be associated with the occurrence of a prepeak in the X-ray and neutron scattering structure function. In a way, although the coordination numbers are different, the behavior of pure MgCl_2 in the crystal and molten states are related in that the lowest q peak is influenced by structural correlations across Mg^{2+} networks. Since we see a mol fraction dependent

coordination number for Mg^{2+} , it would not be surprising if this occurred also for other divalent cationic solutes or even nuclear fuel such as such as UCl_3 , PuCl_3 , UCl_4 . Such behavior could have implications not only for the thermodynamics of the mixture but also for other properties including the reactivity of multivalent ionic solutes. In other words, changes in salt mol fraction could not only affect thermal or transport properties but also possibly solute chemistry.

ASSOCIATED CONTENT

Supporting Information.

The following files are available free of charge on the xxxxxxxx at DOI: xxxxxxxxxxxxxx

AUTHOR INFORMATION

*Email: ivanova@ornl.gov, bryantsevv@ornl.gov, claudio-margulis@uiowa.edu

Notes

The authors declare no competing financial interests.

Acknowledgments

This work was supported as part of the Molten Salts in Extreme Environments Energy Frontier Research Center, funded by the U.S. Department of Energy Office of Science. BNL and ORNL are operated under DOE contracts DE-SC0012704 and DE-AC05-00OR22725, respectively. This research used resources of the Advanced Photon Source operated by Argonne National Laboratory under Contract No. DE-AC02-06CH11357, and the X-ray Pair Distribution Function (PDF; 28-ID-1) beamline of the National Synchrotron Light Source II, a U.S. Department of Energy (DOE) Office of Science User Facility operated for the DOE Office of Science by Brookhaven National Laboratory under Contract No. DE-SC0012704 and of the Oak Ridge Leadership Computing Facility at the Oak Ridge National Laboratory supported by the Office of Science of the U.S.

Department of Energy under contract No. DE-AC05-00OR22725. YI was supported by Grant-in-Aid for JSPS Fellows (Grant No. JP17J01006) from the Japan Society for the Promotion of Science. FW and CJM also acknowledge the University of Iowa High Performance Computing Facility.

REFERENCES

1. Macpherson, H. G. The Molten-Salt Reactor Adventure. *Nucl Sci Eng* **1985**, *90* (4), 374-380.
2. Mathieu, L.; Heuer, D.; Merle-Lucotte, E.; Brissot, R.; Le Brun, C.; Liatard, E.; Loiseaux, J. M.; Meplan, O.; Nuttin, A. Possible Configurations for the Thorium Molten Salt Reactor and Advantages of the Fast Nonmoderated Version. *Nucl Sci Eng* **2009**, *161* (1), 78-89.
3. Liu, J. B.; Chen, X.; Qiu, Y. H.; Xu, C. F.; Schwarz, W. H. E.; Li, J. Theoretical Studies of Structure and Dynamics of Molten Salts: The LiF-ThF₄ System. *J Phys Chem B* **2014**, *118* (48), 13954-13962.
4. Mathieu, L.; Heuer, D.; Brissot, R.; Garzenne, C.; Le Brun, C.; Lecarpentier, D.; Liatard, E.; Loiseaux, J. M.; Meplan, O.; Merle-Lucotte, E.; Nuttin, A.; Walle, E.; Wilson, J. The thorium molten salt reactor: Moving on from the MSBR. *Prog Nucl Energy* **2006**, *48* (7), 664-679.
5. Nuttin, A.; Heuer, D.; Billebaud, A.; Brissot, R.; Le Brun, C.; Liatard, E.; Loiseaux, J. M.; Mathieu, L.; Meplan, O.; Merle-Lucotte, E.; Nifenecker, H.; Perdu, F.; David, S. Potential of thorium molten salt reactors: Detailed calculations and concept evolution with a view to large scale energy production. *Prog Nucl Energy* **2005**, *46* (1), 77-99.
6. Gat, U.; Engel, J. R. Non-proliferation attributes of molten salt reactors. *Nucl Eng Des* **2000**, *201* (2-3), 327-334.
7. Serp, J.; Allibert, M.; Benes, O.; Delpech, S.; Feynberg, O.; Ghetta, V.; Heuer, D.; Holcomb, D.; Ignatiev, V.; Kloosterman, J. L.; Luzzi, L.; Merle-Lucotte, E.; Uhlir, J.; Yoshioka, R.; Dai, Z. M. The molten salt reactor (MSR) in generation IV: Overview and perspectives. *Prog Nucl Energy* **2014**, *77*, 308-319.
8. Delpech, S.; Cabet, C.; Slima, C.; Picard, G. S. Molten fluorides for nuclear applications. *Mater Today* **2010**, *13* (12), 34-41.
9. LeBlanc, D. Molten salt reactors: A new beginning for an old idea. *Nucl Eng Des* **2010**, *240* (6), 1644-1656.
10. Yang, I. H.; Yang, H. C.; Kim, H. J. The Effect of Menisci on Kinetic Analysis of Evaporation for Molten Alkali Metal Salts (CsNO₃, CsCl, LiCl, and NaCl) in Small Cylindrical Containers. *J Chem-Ny* **2018**.
11. Serrano-Lopez, R.; Fradera, J.; Cuesta-Lopez, S. Molten salts database for energy applications. *Chem Eng Process* **2013**, *73*, 87-102.
12. Tukimon, M. F.; Muhammad, W. N. A. W.; Mohamad, M. N. A.; Yusof, F. Characterization and Thermal Properties of Nitrate Based Molten Salt for Heat Recovery System. *J Phys Conf Ser* **2017**, *914*.
13. Wang, J. M.; Jiang, Y. M.; Ni, Y. F.; Wu, A. J.; Li, J. Investigation on static and dynamic corrosion behaviors of thermal energy transfer and storage system materials by molten salts in concentrating solar power plants. *Mater Corros* **2019**, *70* (1), 102-109.

14. Moriyama, H.; Sagara, A.; Tanaka, S.; Moir, R. W.; Sze, D. K. Molten salts in fusion nuclear technology. *Fusion Eng Des* **1998**, 39-40, 627-637.
15. Le Brun, C. Molten salts and nuclear energy production. *J Nucl Mater* **2007**, 360 (1), 1-5.
16. Xu, X. K.; Wang, X. X.; Li, P. W.; Li, Y. Y.; Hao, Q.; Xiao, B.; Elsentriecy, H.; Gervasio, D. Experimental Test of Properties of KCl-MgCl₂ Eutectic Molten Salt for Heat Transfer and Thermal Storage Fluid in Concentrated Solar Power Systems. *J Sol Energ-T Asme* **2018**, 140 (5).
17. Sahoo, D. K.; Singh, H.; Krishnamurthy, N. ELECTROCHEMICAL DEPOSITION OF La-Mg ALLOYS IN LaCl₃-MgCl₂-KCl SYSTEM WITH MOLTEN SALT ELECTROLYSIS PROCESS. *J Min Metall B* **2014**, 50 (2), 109-114.
18. Polimeni, S.; Binotti, M.; Moretti, L.; Manzolini, G. Comparison of sodium and KCl-MgCl₂ as heat transfer fluids in CSP solar tower with sCO₂ power cycles. *Sol Energy* **2018**, 162, 510-524.
19. Dunlop, T. O.; Jarvis, D. J.; Voice, W. E.; Sullivan, J. H. Stabilization of molten salt materials using metal chlorides for solar thermal storage. *Sci Rep-Uk* **2018**, 8.
20. Diamond, D. J.; Brown, N. R.; Denning, R.; Bajorek, S. *Phenomena Important in Molten Salt Reactor Simulations*; BNL-114869-2017-INRE United States 10.2172/1436452 BNL English; ; Brookhaven National Laboratory (BNL), Upton, NY (United States): 2018; p Medium: ED; Size: 85 p.
21. Forsberg, C. W. *Thermal- and fast-spectrum molten salt reactors for actinide burning and fuel production*. American Nuclear Society - ANS, La Grange Park (United States); American Nuclear Society, 555 North Kensington Avenue, La Grange Park, IL 60526 (United States): 2007; p Medium: X; Size: page(s) 1214-1225.
22. Bulmer, J. J. *Fused salt fast breeder: reactor design and feasibility study*. United States Atomic Energy Commission, Technical Information Service Extension: Oak Ridge, Tenn., 1957; p p. 5-214.
23. McMurray, J. W.; Besmann, T. M.; Ard, J.; Fitzpatrick, B.; Piro, M.; Jerden, J.; Williamson, M.; Collins, B. S.; Betzler, B. R.; Qualls, A. L. *Multi-Physics Simulations for Molten Salt Reactor Evaluation: Chemistry Modeling and Database Development*; ORNL/SPR-2018/864 United States 10.2172/1492183 ORNL English; ; Oak Ridge National Lab. (ORNL), Oak Ridge, TN (United States): 2018; p Medium: ED; Size: 91 p.
24. McMurray, J. W.; Besmann, T. M. *Thermodynamic Modeling of Nuclear Fuel Materials*. Springer International Publishing, Basel, Switzerland; Oak Ridge National Lab. (ORNL), Oak Ridge, TN (United States): 2018; p Medium: X; Size: 1.
25. Salanne, M.; Simon, C.; Turq, P.; Madden, P. A. Calculation of Activities of Ions in Molten Salts with Potential Application to the Pyroprocessing of Nuclear Waste. *The Journal of Physical Chemistry B* **2008**, 112 (4), 1177-1183.
26. Austen Angell, C.; Ansari, Y.; Zhao, Z. Ionic Liquids: Past, present and future. *Faraday Discuss.* **2012**, 154, 9-27.
27. Dai, S.; Toth, L. M.; Del Cul, G. D.; Metcalf, D. H. Solubilities of Uranium(IV) Dioxide in Magnesium Chloride, Calcium Chloride, and Aluminum Chloride Melts: A Comparative Study. *The Journal of Physical Chemistry* **1996**, 100 (1), 220-223.
28. Biggin, S.; Gay, M.; Enderby, J. E. The Structures of Molten Magnesium and Manganese(Ii) Chlorides. *J Phys C Solid State* **1984**, 17 (6), 977-985.
29. Wilson, M.; Madden, P. A. Short-Range and Intermediate-Range Order in Mcl₂ Melts - the Importance of Anionic Polarization. *J Phys-Condens Mat* **1993**, 5 (37), 6833-6844.

30. Balasubrahmanyam, K. Raman Spectra of Liquid MgCl₂ and Liquid MgCl₂-KCl System. *J Chem Phys* **1966**, *44* (9), 3270-+.
31. Capwell, R. J. Raman Spectra of Crystalline and Molten MgCl₂. *Chem Phys Lett* **1972**, *12* (3), 443-&.
32. Brooker, M. H. Raman Spectroscopic Study of Structural Aspects of K₂MgCl₄ and Cs₂MgCl₄ as Solid Single-Crystals and Molten-Salts. *J Chem Phys* **1975**, *63* (7), 3054-3061.
33. Huang, C. H.; Brooker, M. H. Raman-Spectrum of Molten MgCl₂. *Chem Phys Lett* **1976**, *43* (1), 180-182.
34. Maroni, V. A.; Hathaway, E. J.; Cairns, E. J. Structural Studies of Magnesium Halide-Potassium Halide Melts by Raman Spectroscopy. *J Phys Chem-US* **1971**, *75* (1), 155-&.
35. Brooker, M. H.; Huang, C. H. Raman-Spectroscopic Studies of Structural-Properties of Solid and Molten States of the Magnesium-Chloride Alkali-Metal Chloride System. *Can J Chem* **1980**, *58* (2), 168-179.
36. Maroni, V. A. Vibrational Frequencies and Force Constants for Tetrahedral MgX₄-2 (X=Cl, Br, and I) in MgX₂-KX Melts. *J Chem Phys* **1971**, *55* (10), 4789-&.
37. Dai, S.; Begun, G. M.; Young, J. P.; Mamantov, G. Application of Chemometric Methods in Raman-Spectroscopic Studies of Molten-Salt System Containing MgCl₂-KCl - Experimental-Evidence for Existence of Mg₂Cl₇³⁻ Dimer and Its Raman-Spectrum. *J Raman Spectrosc* **1995**, *26* (10), 929-932.
38. Ohtori, N.; Salanne, M.; Madden, P. A. Calculations of the thermal conductivities of ionic materials by simulation with polarizable interaction potentials. *J Chem Phys* **2009**, *130* (10).
39. Ishii, Y.; Kasai, S.; Salanne, M.; Ohtori, N. Transport coefficients and the Stokes-Einstein relation in molten alkali halides with polarisable ion model. *Mol Phys* **2015**, *113* (17-18), 2442-2450.
40. Salanne, M.; Simon, C.; Turq, P.; Madden, P. A. Heat-transport properties of molten fluorides: Determination from first-principles. *J Fluorine Chem* **2009**, *130* (1), 38-44.
41. Annapureddy, H. V. R.; Kashyap, H. K.; De Biase, P. M.; Margulis, C. J. What is the Origin of the Prepeak in the X-ray Scattering of Imidazolium-Based Room-Temperature Ionic Liquids? *J Phys Chem B* **2010**, *114* (50), 16838-16846.
42. Kashyap, H. K.; Santos, C. S.; Daly, R. P.; Hettige, J. J.; Murthy, N. S.; Shirota, H.; Castner, E. W.; Margulis, C. J. How Does the Ionic Liquid Organizational Landscape Change when Nonpolar Cationic Alkyl Groups Are Replaced by Polar Isoelectronic Diethers? *J Phys Chem B* **2013**, *117* (4), 1130-1135.
43. Araque, J. C.; Hettige, J. J.; Margulis, C. J. Modern Room Temperature Ionic Liquids, a Simple Guide to Understanding Their Structure and How It May Relate to Dynamics. *J Phys Chem B* **2015**, *119* (40), 12727-12740.
44. Kashyap, H. K.; Hettige, J. J.; Annapureddy, H. V. R.; Margulis, C. J. SAXS anti-peaks reveal the length-scales of dual positive-negative and polar-apolar ordering in room-temperature ionic liquids. *Chem Commun* **2012**, *48* (42), 5103-5105.
45. Hettige, J. J.; Kashyap, H. K.; Margulis, C. J. Communication: Anomalous temperature dependence of the intermediate range order in phosphonium ionic liquids. *J Chem Phys* **2014**, *140* (11).
46. Schultz, A. J.; Hall, C. K.; Genzer, J. Obtaining concentration profiles from computer simulation structure factors. *Macromolecules* **2007**, *40* (8), 2629-2632.

47. Hettige, J. J.; Araque, J. C.; Margulis, C. J. Bicontinuity and multiple length scale ordering in triphilic hydrogen-bonding ionic liquids. *J Phys Chem B* **2014**, *118* (44), 12706-16.
48. Wu, F.; Karunaratne, W. V.; Margulis, C. J. Ionic Liquid Mixture at the Vacuum Interface and the Peaks and Antipeaks Analysis of X-ray Reflectivity. *J Phys Chem C* **2019**, *123* (8), 4914-4925.
49. Dhungana, K. B.; Faria, L. F. O.; Wu, B. N.; Liang, M.; Ribeiro, M. C. C.; Margulis, C. J.; Castner, E. W. Structure of cyano-anion ionic liquids: X-ray scattering and simulations. *J Chem Phys* **2016**, *145* (2).
50. Santos, C. S.; Annapureddy, H. V. R.; Murthy, N. S.; Kashyap, H. K.; Castner, E. W.; Margulis, C. J. Temperature-dependent structure of methyltributylammonium bis(trifluoromethylsulfonyl) amide: X ray scattering and simulations. *J Chem Phys* **2011**, *134* (6).
51. Partin, D. E.; Okeeffe, M. The Structures and Crystal-Chemistry of Magnesium-Chloride and Cadmium Chloride. *J Solid State Chem* **1991**, *95* (1), 176-183.
52. Biggin, S.; Enderby, J. E. Comments on the Structure of Molten-Salts. *J Phys C Solid State* **1982**, *15* (11), L305-L309.
53. Wilson, M.; Madden, P. A. Anion Polarization and the Stability of Layered Structures in Mx2 Systems. *J Phys-Condens Mat* **1994**, *6* (1), 159-170.
54. McGreevy, R. L.; Pusztai, L. The Structure of Molten Salts. *Proceedings of the Royal Society A: Mathematical, Physical and Engineering Sciences* **1990**, *430* (1878), 241-261.
55. Adya, A. K.; Takagi, R.; Gaune-Escard, M. Unravelling the Internal Complexities of Molten Salts. *Zeitschrift für Naturforschung A* **1998**, *53* (12).
56. McGreevy, R. L. Structure and Dynamics of Molten-Salts - Recent Experimental Advances. *Nuovo Cimento D* **1990**, *12* (4-5), 685-701.
57. Pusztai, L.; McGreevy, R. L. The structure of molten ZnCl₂ and MgCl₂. *J Phys-Condens Mat* **2001**, *13* (33), 7213-7222.
58. Rollet, A. L.; Salanne, M. Studies of the local structures of molten metal halides. *Annu Rep Prog Chem C* **2011**, *107*, 88-123.
59. Hoyer, W.; Neumann, H.; Wobst, M. Structure Investigation on Liquid Tellurium by X-Ray and Neutron-Scattering. *Z Naturforsch A* **1992**, *47* (7-8), 833-840.
60. Proffen, T.; Billinge, S. J. L. PDFFIT, a program for full profile structural refinement of the atomic pair distribution function. *J Appl Crystallogr* **1999**, *32*, 572-575.
61. Akdeniz, Z.; Tosi, M. P. Stability Diagrams for Fourfold Coordination of Polyvalent Metal-Ions in Molten Mixtures of Halide Salts. *J Phys-Condens Mat* **1989**, *1* (13), 2381-2394.
62. Rovere, M.; Tosi, M. P. Structure and Dynamics of Molten-Salts. *Rep Prog Phys* **1986**, *49* (9), 1001-1081.